Theor Chem Acc (2010) 126:177–183
DOI 10.1007/s00214-009-0626-9

REGULAR ARTICLE

Modeling hole transfer in DNA. II. Molecular basis of charge transport in the DNA chain

Daniel Roca-Sanjuán · Gloria Olaso-González · Pedro B. Coto · Manuela Merchán · Luis Serrano-Andrés

Received: 3 June 2009 / Accepted: 10 August 2009 / Published online: 27 August 2009

Abstract A theoretical multiconfigurational second-order perturbation method, CASPT2, has been employed to determine the binding energies and electronic couplings for all pairs of stacked canonical nucleobases in the standard conformation of the B-DNA. The existence and relevance of conical intersections mediating the hole transfer process has been shown in different systems in vacuo and, by using hybrid QM/MM techniques, in a more realistic biological environment, formed by a double helix of 18 oligomers of DNA surrounded by water molecules. The present results support, therefore, the cooperative micro-hopping mechanism proposed in a previous work for the migration of the hole between adjacent π-stacked 2′-deoxycytidine 5′-monophosphate (dCMP) or alternate 2′-deoxyadenosine 5′-monophosphate and dCMP oligonucleotides.

Keywords DNA · Charge transport · Electron transfer · Hole transfer · CASPT2 · Conical intersection · Electronic coupling

1 Introduction

Charge transport (CT) has been described in DNA by studying migration of a previously generated positive or negative charge up to long distances through the π-stacked structure of DNA double helix. The phenomenon can be characterized as hole transport (HT) and excess electron transport, respectively. Ionizing radiation and highly oxidative or reductive endogenous and exogenous chemical compounds are common sources for the creation of charge holes or excess electrons, taking place basically on nucleic acid bases (NABs). Because of its biological implications (charge concentration spots may induce mutations) and its medical and technological applications, CT in DNA is currently the subject of intense experimental and theoretical research [1–3]. However, the detailed mechanism on how a charge migrates between the initial and final charged NABs along the strand is not yet known, and many different hypotheses have been suggested [4]. Among the different proposals put forward, the one that takes place between adjacent NABs is gaining interest. We have recently proposed a cooperative micro-hopping mechanism involving consecutively two-by-two adjacent π-stacked NABs for HT along single strands of only 2′-deoxycytidine 5′-monophosphate (dCMP) or alternate 2′-deoxyadenosine 5′-monophosphate and dCMP oligonucleotides (see Fig. 1) [4]. According to our findings, conical intersections (CIs) and electronic couplings (H′) control the HT process, considered as a typical electron transfer (eT) phenomena [5] that will proceed in a cascade mechanism by means of a thermally activated increase of the intermonomer distance.

Considering a scale of short DNA stacks, the relevance of π-stacking in the efficiency of CT is registered, via the electronic donor–acceptor coupling, in the different models proposed in the literature [1]. Whereas several distinct magnitudes are used in the phenomenological expressions, all the models try to evaluate the perturbation of the nucleobase-charged state by the interaction with the π system of the adjacent bases. That the large-range electrostatic interactions of the acceptor and donor with the surrounding medium could also modulate the rate of CT

Dedicated to the memory of Professor Jean-Pierre Daudey and published as part of the Daudey Memorial Issue.

D. Roca-Sanjuán · G. Olaso-González · P. B. Coto · M. Merchán · L. Serrano-Andrés (✉)
Instituto de Ciencia Molecular, Universitat de València, Apartado 22085, 46071 Valencia, Spain
e-mail: Luis.Serrano@uv.es

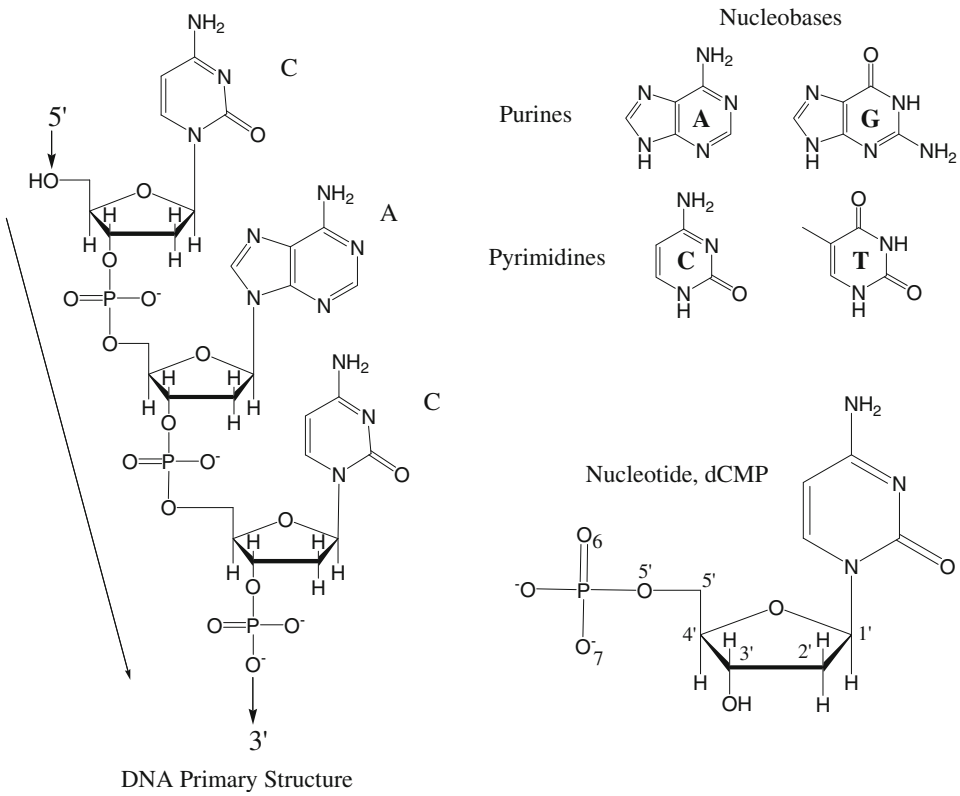

Fig. 1 The structure of DNA and its components: the nucleic acid bases adenine (*A*), guanine (*G*), cytosine (*C*) and thymine (*T*) (*right and top*), the 2′-deoxycytidine 5′-monophosphate (*dCMP*) nucleotide (*right and bottom*) and a single strand of alternate dCMP and 2′-deoxyadenosine 5′-monophosphate (*dAMP*) oligonucleotides, indicating the orientation 5′–3′of the chain (*left*)

and some mechanisms proposed in the bibliography are based on these [6–8].

This contribution is an extension of our previous work based on modeling hole transfer in DNA [4], supporting the mechanism suggested there for the migration of a charge through the double helix and analysing the efficiency of CT. We show here by using the well-established complete-active-space self-consistent-field second-order perturbation theory (CASPT2) [9] that the existence of CIs mediating the HT process is possible at geometries close to the common structure of B-DNA. Electronic couplings computed using an energy gap-based method such as supermolecule dimer approach in a quasi-diabatic regime is employed, as it was shown previously to be convenient and accurate [10–12]. The calculations are done for the different combinations (homodimers and heterodimers) of the four natural isolated DNA NABs, and also include results obtained in a double helix of 18 pairs of alternate C·G and T·A oligonucleotides surrounded by water molecules, by means of a QM/MM procedure. Therefore, it takes into account the effect of the environment in the HT process between two nucleobases.

2 Methods and computational details

Characterization of the two lowest doublet states of the 16 possible nucleobases dimers was carried out in vacuo, by using the CASPT2 quantum chemical method as implemented in the MOLCAS 7.0 software [13, 14]. The standard parameters of B-DNA were used for the geometry of each monomer and for the arrangements of dimers [15, 16]. To minimize weakly interacting intruder states, the imaginary level-shift technique (0.2 au) was employed [17]. With the aim of comparing with previously determined calculations on NABs cations, the CASPT2 calculations were performed including the IPEA correction with a selected value of 0.25 au [18]. The basis set of atomic natural orbital (ANO-S) type with the primitive set C,N,O(10s6p3d)/H(7s3p), contracted to C,N,O[3s2p1d]/H[2s1p], was used throughout. The active space for the CASSCF wave functions comprises a total of 12 electrons distributed along 12 π molecular orbitals (MOs), CASSCF(12/12), which correspond to 6 MOs of each nucleobase. Lone-pair orbitals and electrons play a minor role in describing the π-stacked DNA pairs, since they would be mainly involved in interactions through hydrogen bonds with the water molecules and other NABs, as in the Watson–Crick pairs. The inclusion of the basis set superposition error (BSSE) is crucial to accurately describe the binding energies. The effect was taken into account by using the counterpoise correction (CP). The corrected counterpoise binding energy was denoted by E_b [4]. The CIs $(D_1/D_0)_{CI}$ were initially computed as CASSCF minimum energy crossing points by using the restricted

Lagrange multipliers technique as included in the MOLCAS-7.0 package, in which the lowest energy point was obtained under the restriction of degeneracy between the two considered states. The structures were later computed at the CASPT2 level.

The influence of the environment was evaluated by using the QM/MM scheme that employed as quantum chemical core, the ab initio CASPT2//CASSCF approach. The employed QM/MM strategy [19] was based on a standard electrostatic embedding approach, using a hydrogen link atom scheme to describe the frontier region placed at the glycosidic bond of the nucleoside. The MM subsystem was represented using the AMBER99 forcefield [20]. Both subsystems (QM and MM) interact in the following way: (a) the QM wave function is polarized by all the MM point charges; (b) stretching, bending and torsion potentials involving at least one MM atom are described at the MM level; (c) standard van der Waals potentials are used to represent the interaction between atom pairs (QM/MM) separated by more than two bonds. Therefore, the Hamiltonian used in the computations takes the following form:

$$\hat{H} = \hat{H}_{QM} + \hat{H}_{MM} - \sum_{i=1}^{n}\sum_{j=1}^{Q}\frac{q_j}{r_{ij}} + \sum_{i=1}^{N}\sum_{j=1}^{Q}\frac{Z_i q_j}{R_{ij}} + E_{vdW} + E_{Frontier} \quad (1)$$

where $\hat{H}_{QM}$ is the Hamiltonian of the QM subsystem in vacuo, $\hat{H}_{MM}$ is the Hamiltonian of the MM subsystem computed using the AMBER forcefield, and the remaining four terms are the interacting QM/MM Hamiltonian, with the first two terms comprising the electrostatic interactions [polarization of the wavefunction by the MM charges and Coulomb term between QM and MM nuclei, which in the optimizations carried out were approximated using the ESPF method (electrostatic potential fitted operator method [21])], the third one corresponding to the van der Waals interaction term computed using the definition of the AMBER forcefield, and the last one containing the terms needed for a proper description of the frontier within the hydrogen link atom scheme. Within this model, the MM charges remain constant through the computation, and no polarization of the MM region is taken into account with an explicit term (yet polarization is included in a mean-field way in the parametrization of the AMBER point charges). During the optimizations, the MM region surrounding the QM subsystem within 5 Å was allowed to relax using the microiterations technique (see, e.g., reference [22]). Examples of successful QM/MM applications on fast chemical processes in biological compounds can be found in the literature [23, 24] All the new computations reported here were carried out using the 7.3 version of the MOLCAS package.

3 Results and discussion

3.1 Electronic coupling

The calculation of the electronic coupling matrix element H′ is the crucial part in the determination of eT rates and lifetimes. The extent of the coupling controls the eT process, specifically the passage from one state to another and it can be taken as a measure of its efficiency. Different procedures to estimate the eT coupling have been developed [25–27] based on diabatic localized dimer calculations, monomer transition densities or transition dipole moments, and a supermolecule ansatz of the dimer [25]. From all procedures, we will employ an energy gap-based method, such as supermolecule dimer approach, in which the value of the coupling is obtained as half of the splitting or perturbation between the interacting states, shown previously to be convenient to analyze comparatively the extent of eT process in related compounds [12].

In this case, the two situations considered are the non-interacting monomers (separated by 10 Å), in which the energy difference corresponds to that of the ionization potentials (IPs) of the pair of NABs (|ΔIP|), and the B-DNA arrangement. The energy difference is coined as ΔE_{BDNA}. Therefore, the computed electronic coupling is obtained as $1/2\ |\Delta E_{\mathrm{BDNA}} - |\Delta \mathrm{IP}||$. It is clear that the accuracy of the procedure strongly relies on the quality of the quantum chemical method used to perform the electronic structure calculations, something guaranteed in the present study by the highly reliable and accurate CASPT2 method. Additionally, we successfully calibrated the present results with respect to our previous benchmark calculations on the IPs of the nucleobases [19, 28–30]. Notice that the BSSE problem does not affect the results of the coupling, which uses energy differences between states computed at the same geometry [12].

Table 1 compiles the BSSE corrected binding energies (E_b), with respect to their respective asymptotic limit and the electronic coupling (H′) of all possible pairs of NABs that can be found in the standard B form of DNA. Since canonical DNA is a double helix where each pair of adjacent nucleobases are twisted to 36° [16], two different dispositions of two NABs are possible in a dimer, depending on the position of each NAB at the extreme 3′ or 5′ (see Fig. 1). Both, the values of the binding energies, E_b, and the electronic coupling (H′), are extremely sensitive to the 3′–5′ or 5′–3′ arrangement. Considering the homodimers, while the position of the hole is more stable at the 3′ extreme of the DNA strand in adenine and cytosine, the 5′ position has preference in guanine and thymine. The results agree with the theoretical studies of Blancafort and Voityuk [31] and support previous experimental evidence. It is shown that adjacent guanine nucleobases give rise to

Table 1 Energy differences (all in eV) between the two lowest-energy doublet states of the positively charged π-stacked nucleobases for the non-interacting monomers ($|\Delta IP|$) and at the B-DNA arrangement (ΔE_{BDNA}), BSSE-corrected E_b binding energies with respect to the corresponding monomer IP at the B-DNA conformation, and computed electronic coupling (H′)

$[X_{3'}Y_{5'}]^+$	$\|\Delta IP\|$	E_b		ΔE_{BDNA}	H′[b]
		$X^+_{3'} - Y_{5'}$	$X_{3'} - Y^+_{5'}$		
AA	0.00	0.56	0.37	0.19	0.095
AC	0.03	0.41	0.21	0.23	0.100
AG	0.54	0.43	0.56	0.67	0.068
AT	0.67	0.23	0.26	0.63	0.020
CA[a]	0.03	0.48	0.26	0.19	0.080
CC	0.00	0.35	0.06	0.29	0.145
CG	0.61	0.41	0.61	0.81	0.100
CT	0.62	0.25	0.10	0.77	0.075
GA	0.54	0.56	0.70	0.40	0.070
GC	0.61	0.73	0.72	0.62	0.005
GG	0.00	0.30	0.57	0.27	0.135
GT	1.13	0.27	0.69	0.72	0.206
TA	0.67	0.26	0.28	0.69	0.001
TC	0.62	0.50	0.28	0.40	0.110
TG	1.13	0.20	0.31	1.24	0.055
TT	0.00	0.14	0.42	0.28	0.140

[a] In this arrangement, the states change order from that of the non-interacting monomers

[b] Computed as $H' = 1/2\ |\Delta E_{BDNA} - |\Delta IP||$. See text

potential energy wells where the positive hole can be trapped and this charge is located at the 5′ extreme [32], according to our results (see Table 1). In the case of the heterodimers, the largest values of E_b imply the presence of guanine at the 3′ extreme, contrary to the homodimer $[G_{3'}G_{5'}]^+$, whereas thymine appears in the charged heterodimers with the lowest E_b.

In the homodimers, the coupling represents directly the degree of interactions between the two lowest states of the cation. By decreasing the intermonomer distance, it varies from the exciton-type point (where the degeneracy is broken [4]) toward the B-DNA arrangement, taking place at shorter distances (average of 3.4 Å). At such conformation, the computed binding energies follow the expectations, being larger for purine than for pyrimidine NABs for the two states. This means that both situations (charge localized in each monomer) are strongly stabilized in purines by the interaction of the stacked bases. Previous models showed purine NABs, in particular guanine, as series of adjacently stacked NABs that stabilized the positive charge and behaved as a well, whereas pyrimidine NABs behaved as a wall [32]. Indeed, the more the number of equivalent adjacent NABs present in the sequence of oligonucleobases, the larger will be the stabilization of the charged states in purines in contrast to pyrimidines. With respect to the value of the electronic coupling, it is closely related to the behavior previously reported. Pyrimidine NABs show relatively large couplings (near 0.14 eV), whereas those of the purine NABs are slightly smaller. This means that the states become closer in energy. As the coupling is the driving force allowing the transfer of charge from one monomer to the other, one should initially conclude that this is more favorable in homodimers for pyrimidine than for purine NABs. Regarding the heterodimers, the largest values for the electronic coupling are those corresponding to the pair $[G_{3'}T_{5'}]^+$, related to the combination of NABs, which most differ in their IPs (see ΔIP in Table 1). In the case of the $[C_{3'}A_{5'}]^+$ arrangement, the states change order from the most favorable localization of the hole in adenine for the isolated systems to that on the cytosine at the B-DNA structure. In most cases, however, the magnitude of the coupling is not as large as for the homodimers. As we will show later, there are structures more favorable for charge transfer in heterodimers than that of B-DNA. The coupling, on the other hand, does not directly inform about the direction of the transfer, but becomes an indication of the tendency of the system to transfer charge between two entities, which use as a driving force for the process the distinct tendency for oxidation. The transfer of the charge has, however, to balance two factors: electronic coupling and resonance condition. How important the energy difference and the structure between the interacting moieties can be for the charge transfer process? We have computed several cases to illustrate this point, discussed in the next subsection.

3.2 Conical intersections

The essential role of CIs mediating the HT process was highlighted in our previous work [4]. By building the vertical potential energy curves at the CASPT2 level of theory with respect to the rise parameter, a crossing point was located in the two lowest doublet states of the positively charged cytosine homodimer in both, the face-to-face (CC^+) and B-DNA ($[C_{3'}C_{5'}]^+$) forms of arrangements. In the highly stacked CC^+ dimer, the degeneracy between the states C^+–C y C–C^+, which have the hole in each monomer, begin at 5.0–5.5 Å. This point occurs even at larger distances for the B-DNA arrangement. Such degeneracy point (CI) will not have the same meaning for homodimers and heterodimers. In the CI, the electronic coupling will be exactly half of the energy difference between the IPs of the NABs, and therefore it will be 0 for the homodimers. It can be understood that at the CI the system of equivalent monomers has no preference between the two states, since they are identical. The probability of charge transfer will be larger in those cases

at different geometries, for instance, at shorter intermonomer distances. In the heterodimers, however, the coupling will be, also at the CIs, proportional to the difference between the monomers IPs, and therefore the transfer probability will be most favorable by the combination of both factors, strength of the coupling and resonance condition. Again, the GT pairs will represent the most efficient case.

In the case of the heterodimer $[C_{3'}A_{5'}]^+$, it was shown [4] that by decreasing the intermonomer distance in the B-DNA arrangement, the low-lying states changed order and the crossing point was placed at 5.5–6.0 Å. Below 4.0 Å, the energy difference between the doublet states is already lower than 0.1 eV, which imply a more favorable situation for the process of hole migration with respect to the cytosine homodimer. In that study, only the *rise* was taken into account as the structural parameter driving the HT process, but in DNA many other possible helicoidal motions between two adjacent NABs exist. Here, we carried out the search for CIs in vacuo with no constraints to the relative orientation between NABs in three different systems: $[G_{3'}A_{5'}]^+$, $[G_{3'}C_{5'}]^+$ and $[G_{3'}T_{5'}]^+$. All of them contain guanine, the NAB with the lowest IP [28], at the 3′ position and one of the other B-DNA bases at the 5′ extreme. The absence of geometrical restrictions allows even unphysical structures of the bases, such as T-shaped ones, for the degeneracy points between the two lowest energy doublet states. Ignoring such arrangements, Fig. 2 displays the obtained CI structure for the $[G_{3'}C_{5'}]^+$ heterodimer, which takes place at a geometry not so different from that of the B-DNA arrangement. Similar conclusions are obtained for the $[G_{3'}A_{5'}]^+$ and $[G_{3'}T_{5'}]^+$ systems, and are expected in other pairs of nucleobases.

Table 2 contains the energies of the two lowest doublet states of the three positively charged heterodimers ($[G_{3'}A_{5'}]^+$, $[G_{3'}C_{5'}]^+$ and $[G_{3'}T_{5'}]^+$) at the B-DNA arrangement and the energy of the corresponding CIs (energies are related to the ground state of the neutral dimer separated at 10 Å). In agreement with guanine being the nucleobase with the lowest IP [28], the lowest doublet state in all three systems at the B-DNA structure corresponds to the location of the hole in this purine base. In all cases, the CI is placed slightly above the lowest state (0.20–0.55 eV), and for the GA and GC pairs close to the second state. A thermally activated DNA chain, undergoing large mechanical motions due to its inherent flexibility, can surmount such type of barriers. In the CI, the combination of large electronic couplings (close to half of the ΔIP between the isolated NABs) and small energy differences will certainly enhance the probability of charge transfer in the heterodimers. Because of the relatively large coupling, the CI structures will be extremely favorable for the GT pair.

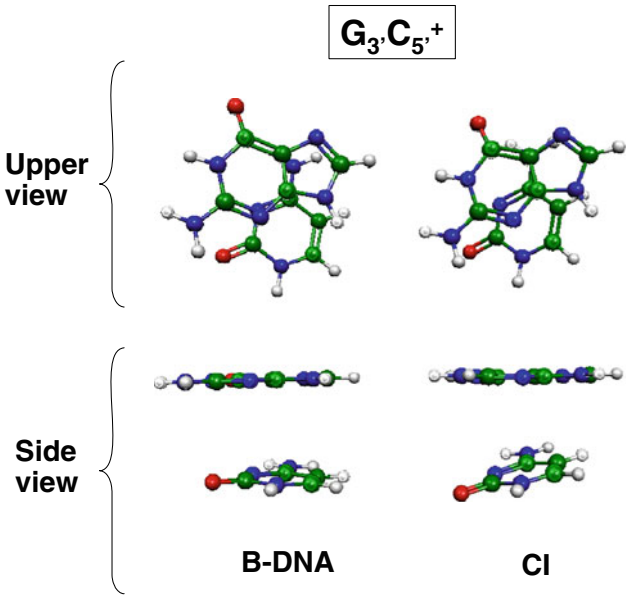

Fig. 2 Two different views of the geometries of the heterodimer $[G_{3'}C_{5'}]^+$ at the standard conformation of B-DNA and at the structure of the computed conical intersection (*CI*)

Table 2 Relative energies of the two lowest doublet states of the heterodimers $[G_{3'}A_{5'}]^+$, $[G_{3'}C_{5'}]^+$ and $[G_{3'}T_{5'}]^+$, at the B-DNA and CI structures, with respect to the energy of the respective neutral dimers at an intermolecular distance (rise) of 10 Å

Dimer	State	E_{rel}/eV	
		B-DNA	CI
$[G_{3'}A_{5'}]^+$	$G_{3'}^+ - A_{5'}$	7.46	7.86
	$G_{3'} - A_{5'}^+$	7.85	
$[G_{3'}C_{5'}]^+$	$G_{3'}^+ - C_{5'}$	7.30	7.85
	$G_{3'} - C_{5'}^+$	7.90	
$[G_{3'}T_{5'}]^+$	$G_{3'}^+ - T_{5'}$	7.74	7.94
	$G_{3'} - T_{5'}^+$	8.46	

Furthermore, in the GT pair, the CI clearly favors the localization of the charge in the guanine moiety, since it is much lower than to the B-DNA relative energy (see Table 2).

3.3 Environmental effects

The stabilization of a charged state in a molecule is affected by the presence of charges surrounding the system. Therefore, in the present context, we can expect that the location of the hole in one or another nucleobase in the dimer can be modulated by interaction with external charges. We carried out at the CASPT2(6,6) level, a Mulliken Population Analysis (MPA) of the ground state of both the neutral and cationic states of thymine, cytosine, adenine and guanine, in the B-DNA standard geometries.

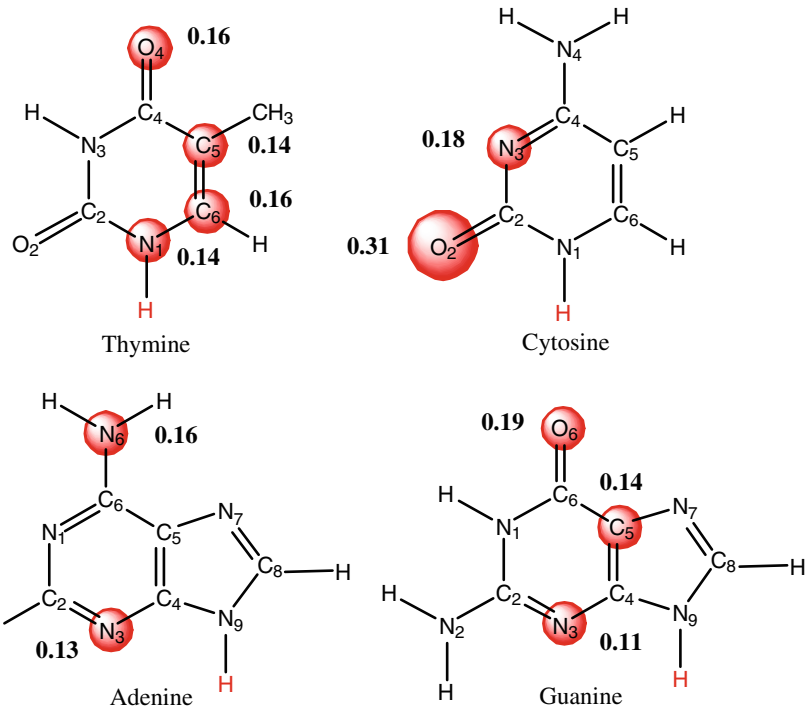

Fig. 3 Differences in the Mulliken Population Analysis (*MPA*) between the neutral and cationic DNA nucleobases. The largest difference between the MPA charges are indicated and the related atom is highlighted. *Red* hydrogen atoms correspond to the site where nucleobases are bound to the sugar moiety in nucleotides

Figure 3 shows the largest difference in the MPA charges between the neutral and cationic NABs. These values are nearly identical to those of the LoProp Population Analysis [33]. While the electronic density is basically extracted from the oxygen atom in cytosine, the atoms O4, N1, C5 and C6 undergo the largest changes in thymine. In the case of purine nucleobases, the positive charge is mainly removed from the nitrogen atoms N3 and N6, in adenine, and from N3, O6, and C9, in guanine.

Taking into account the MPA and to study the influence of external charges in the stability of the two lowest doublet states of the dimers of NABs, a series of calculations were undertaken on the $[G_{3'}C_{5'}]^+$ system, placing a negative charge at different distances from the oxygen atom O2 of cytosine, as indicated in Fig. 4. The result of these computations (see Fig. 4) confirms our hypothesis on the effect of external charges in the location of the hole. Thus, while the point charge is far from the dimer, the lowest doublet state corresponds to $G^+_{3'} - C_{5'}$ (the hole is located in guanine); but, when the negative charge becomes closer to the O2 atom of cytosine, the energy gap between the doublet states $G^+_{3'} - C_{5'}$ and $G_{3'} - C^+_{5'}$ becomes lower, and at a distance of 3 Å the location of the hole is more favorable in cytosine.

This simple analysis illustrates the sensitivity of the charge transfer process to the interactions between the acceptor and donor target nucleobases and the medium surrounding them in physiological conditions. This factor has to be taken into account in conjunction with the π-stacking to provide a complete description of the phenomenon. Therefore, we carried out preliminar QM/MM

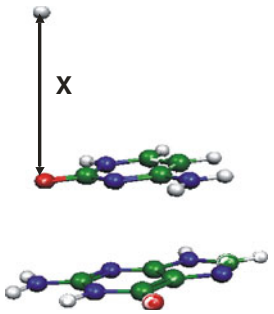

X/Å	Lowest state	ΔE/eV
11	$G_{3'}^{+}$- $C_{5'}$	0.42
6	$G_{3'}^{+}$- $C_{5'}$	0.15
3	$G_{3'}$ - $C_{5'}^{+}$	0.95

Fig. 4 Analysis of the effect of a negative external charge in the stability of the two lowest states of the heterodimer $[G_{3'}C_{5'}]^+$. The values ΔE correspond to the energy difference between the states

calculations to determine the optimized CI structure between the two lowest doublet states of the π-stacked heterodimer cytosine–thymine (C–T) in a double helix of 18 base pairs of alternate C·G and T·A, dressed also with water molecules. The obtained conclusions show that, whereas the structure of the CI for the isolated dimer clearly deviates from the B-DNA conformation, in the more realistic environment of the oligomers, the degeneration between the two doublet states is reached at a structure much closer to that of B-DNA. Although many more simulations should be performed to strengthen this point, a clear conclusion is that the interactions with the environment largely favors the occurrence of the HT process by placing the CI to be more accessible, that is, closer to the average B-DNA structure. Further studies are in their way to confirm this finding.

3.4 Summary and conclusions

The present contribution supports the mechanism suggested by the authors in a previous work based on modeling hole transfer in DNA by means of a micro-hopping transfer between two adjacent π-stacked nucleobases and analyzes the efficiency of the process of migration of a positive charge in terms of the presence of regions of CI and the strength of the electronic coupling between the related states. At the BSSE-corrected CASPT2(IPEA)/ANO-S 321/21 level of theory, the binding energies of the two lowest doublet states and their electronic couplings, computed using an energy-gap method such as supermolecule dimer approach in a quasi-diabatic regime, were determined for the different combinations of the four natural DNA NABs in isolation. The existence of CIs mediating the HT process was studied in three different systems in vacuo: GA, GC and GT, and in the heterodimer C–T embedded in a double helix of 18 pairs of alternate C·G and T·A oligonucleotides surrounded by water molecules, after a detailed analysis of the effect of external charges in the stability of charged states of nucleobases.

In summary, it is concluded that both, binding energies and electronic couplings, are extremely sensitive to the arrangement and to the nucleobase counterpart. Positive values larger than zero for the binding energies prove that stable excimer-like structures are plausible in charged π-stacked dimers. Regarding the electronic coupling, the largest value is found in the pair GT, the nucleobases of which have the largest difference between the respective IPs. This magnitude, H′, is an indication of the tendency of the system to transfer a charge between the moieties, but it has to be balanced with another factor, the resonance condition, that is, the presence of a region of CIs, to provide a complete understanding of the phenomenon of charge migration. In this context, CIs have been located in the system's GA, GC and GT at structures not far from the B-DNA conformation, and with energies near the second doublet state for the GA and GC pairs and between the two lowest states in the case of the GT dimer. The environmental charges surrounding the acceptor and donor nucleobases are also another relevant factor modulating the process of CT along the π structure of the nucleic acid strands. The presence of a single negative charge near the oxygen of cytosine in the heterodimer $[G_{3'}C_{5'}]^+$ makes the $G_{3'} - C^+_{5'}$ state more stable than that characterized by the location of the hole in guanine. When the oligomer structure (18-mer) and the environment are considered by means of a QM/MM approach, the CI between the two lowest states of the pair $[T_{3'}C_{5'}]^+$ is found at a structure even closer to the B-DNA arrangement than in vacuo, making, therefore, the process of HT more favorable in the biological medium.

Acknowledgments The research reported has been financed by projects CTQ2007-61260 and CSD2007-0010 Consolider-Ingenio in Molecular Nanoscience of the Spanish MEC/FEDER. It is a great pleasure for us to dedicate this paper *in memoriam* to Prof. Jean-Pierre Daudey. His scientific teachings and charismatic personality shall always be part of our background.

References

1. Rösch N, Voityuk AA (2004) Top Curr Chem 237:37
2. Delaney S, Barton JK (2003) J Org Chem 68:6475
3. Starikov EB (2000) Int J Quantum Chem 77:859
4. Roca-Sanjuán D, Merchán M, Serrano-Andrés L (2008) Chem Phys 349:188
5. Hsu CP (2009) Acc Chem Res 42:509
6. Voityuk AA, Siriwong K, Rösch N (2001) Phys Chem Chem Phys 3:5421
7. Troisi A, Orlandi G (2002) J Phys Chem B 106:2093
8. Grozema FC, Siebbeles LDA, Berlin YA, Ratner MA (2002) Chemphyschem 3:536
9. Andersson K, Malmqvist PA, Roos BO (1992) J Chem Phys 96:1218
10. Fink RF, Pfister J, Schneider A, Zhao H, Engels B (2008) Chem Phys 343:798
11. You ZQ, Hsu CP, Fleming GR (2006) J Chem Phys 124:44506
12. Serrano-Pérez JJ, Olaso-González G, Merchán M, Serrano-Andrés L (2009) Chem Phys 360:85
13. Karlström G, Lindh R, Malmqvist PA, Roos BO, Ryde U, Veryazov V, Widmark PO, Cossi M, Schimmelpfennig B, Neogrady P, Seijo L (2003) Comput Mater Sci 28:222
14. Veryazov V, Widmark PO, Serrano-Andrés L, Lindh R, Roos BO (2004) Int J Quantum Chem 100:626
15. Chandrasekaran R, Arnott S (1989) In: Saenger W (ed) Science and technology, group VII/1b, nucleic acids. Springer, Berlin, p 31
16. Arnott S (1999) In: Neidle S (ed) Oxford handbook of nucleic acid structure. Oxford University Press, Oxford, p 1
17. Forsberg N, Malmqvist PA (1997) Chem Phys Lett 274:196
18. Ghigo G, Roos BO, Malmqvist PA (2004) Chem Phys Lett 396:142
19. Roca-Sanjuán D, Olaso-González G, Rubio M, Coto PB, Merchán M, Ferré N, Ludwig V, Serrano-Andrés L (2009) Pure Appl Chem 81:743
20. Wang JP, Cieplack P, Kollman PA (2000) J Comput Chem 21:1049
21. Ferré N, Ángyán JG (2002) Chem Phys Lett 356:331
22. Vreven T, Morokuma K, Farkas O, Schlegel HB, Frisch MJ (2003) J Comput Chem 24:760
23. Senn HM, Thiel W (2009) Angew Chem Int Ed Engl 48:1198
24. Strambi A, Coto PB, Frutos LM, Ferré N, Olivucci M (2008) J Am Chem Soc 130:3382
25. Scholes GD, Ghiggino KP (1994) J Chem Phys 101:1251
26. Scholes GD, Harcourt RD (1996) J Chem Phys 104:5054
27. Scholes GD, Harcourt RD, Ghiggino KP (1995) J Chem Phys 102:9574
28. Roca-Sanjuán D, Rubio M, Merchán M, Serrano-Andrés L (2006) J Chem Phys 125:084302
29. Rubio M, Roca-Sanjuán D, Merchán M, Serrano-Andrés L (2006) J Phys Chem B 110:10235
30. Rubio M, Roca-Sanjuán D, Serrano-Andrés L, Merchán M (2009) J Phys Chem B 113:2451
31. Blancafort L, Voityuk AA (2006) J Phys Chem A 110:6426
32. Joseph J, Schuster GB (2006) J Am Chem Soc 128:6070
33. Aquilante F, Vico LD, Ferré N, Ghigo G, Malmqvist PA, Pedersen T, Pitonak M, Reiher M, Roos BO, Serrano-Andrés L, Urban M, Veryazov V, Lindh R (2009) J Comput Chem (in press)